



RESEARCH ARTICLE

APPLICATION OF IRON OXIDE NANOPARTICLES IN THE ADSORPTION OF
CHROMIUM (VI) AND COPPER (II)

¹Shrikrishna, H Gurlhosur, ^{2,*}Sreekanth, B., ³Shashidhar, N., ⁴Rajeshwari Desai,
⁵Amruta Bhusanur, ⁶Chaitanya Puranik and ⁷Sri SaiTejaswini, P.

¹Asst. Prof. Department of Chemical Engineering, Rural Engineering College, Hulkoti

³Shashidhar N Belongs to Department of Chemistry, SDM College of Engg. and Technology, Dharwad,
Karnataka, India

^{2,4,5,6} Sreekanth B and others belongs to Department of Chemical Engineering, SDM College of Engg. and
Technology, Dharwad, Karnataka, India

⁷Department of Chemical Engineering, Rural Engineering College, Hulkoti

ARTICLE INFO

Article History:

Received 21st November, 2017

Received in revised form

27th December, 2017

Accepted 15th January, 2018

Published online 28th February, 2018

Key words:

Fe₃O₄ Nanoparticles,
Co-precipitation,
Adsorption,
Cu(II) & Cr(VI),
Synthetic Wastewater,
Heavy metal removal efficiency.

ABSTRACT

Due to the infinite size of nanoparticles, the surface area is relatively large and as a result, they usually have high reactivity and sorption to various heavy metals. In this work, we synthesized Fe₃O₄ nanoparticles by cost effective Co-precipitation method. The prepared nanoparticles were characterized using Scanning electron microscopy (SEM), X-ray powder diffraction (XRD) and Fourier transform infrared spectroscopy (FTIR). The results from SEM, XRD & FTIR reveals that the synthesized nanoparticles Fe₃O₄ were having spherical shape with the particle size ranging between 8.69nm-56.58nm (<100nm). We investigated the adsorption behavior of the iron oxide (Fe₃O₄) nanoparticles and its applicability in the removal of toxic heavy metals like Copper (Cu-II) and Chromium (Cr-VI). A batch experiment was performed in which 100mL of aqueous solutions contaminated with each metal were artificially prepared from their standard stock solutions and treated with the nanoparticles under different conditions of pH, contact time, dosage Fe₃O₄, metal concentration and temperature. The adsorption behavior was studied using UV-VIS spectrophotometer by changing one of the conditions while keeping the others fixed. According to the results, maximum metal removal Efficiency (%) for Cu(II) & Cr(VI) were obtained at: pH=6 for Cu(II) and pH=2 for Cr(VI); Contact time=60minutes; dosage Fe₃O₄ =0.2grams; Temperature=30°C; Metal concentration=10ppm for Cu(II) & 20ppm for Cr(VI). Langmuir isotherm fits the data having R²=0.997 for Cu(II) & R²=0.996 for Cr(VI) with maximum adsorption capacity (Q₀) of 31.25mg/g for Cu(II) and 55.56mg/g for Cr(VI).

Copyright © 2018, Shrikrishna, H Gurlhosur et al. This is an open access article distributed under the Creative Commons Attribution License, which permits unrestricted use, distribution, and reproduction in any medium, provided the original work is properly cited.

Citation: Shrikrishna, H Gurlhosur, Sreekanth, B., Shashidhar, N., Rajeshwari Desai, Amruta Bhusanur, Chaitanya Puranik and Sri SaiTejaswini, P. 2018. "Application of Iron Oxide Nanoparticles in the Adsorption of Chromium (VI) and Copper (II)", *International Journal of Current Research*, 10, (02), 65995-65999.

INTRODUCTION

Nanoscience is one of the most important research and development frontiers in modern science. Nanotechnology is now widely used throughout the pharmaceutical industry, medicine, electronics, robotics, and tissue engineering. The use of nanoparticles offers many advantages due to their unique smaller size. The superparamagnetic nano particles is one of these nanoparticles, which can be manipulated by an external magnetic field to lead it to the target tissue (Prijić and Sersa, 2011). Based on their unique mesoscopic physical, chemical, thermal, and mechanical properties, superparamagnetic nanoparticles offer a high potential for several biomedical applications, such as: (a) cellular therapy such as cell labeling, targeting and as a tool for cell-biology research to separate and purify cell populations; b) tissue repair; (c) magnetic field-

guided carriers for (localizing drugs or radioactive therapies; (d) magnetic resonance imaging (MRI); (e) tumor hyperthermia; (f) magnetofection. Furthermore, special surface coating of the magnetic particles require, which has to be not only non-toxic and biocompatible but also allow a targetable delivery with particle localization in a specific area. Magnetic nanoparticles can bind to drugs, proteins, enzymes, antibodies, or nucleotides and can be directed to an organ, tissue, or tumor using an external magnetic field or can be heated in alternating magnetic fields for use in hyperthermia. The heavy metal pollution is becoming one of the most serious environmental problems. Therefore various methods for heavy metal removal from wastewater have been extensively studied during the past decades, such as chemical precipitation, electrochemical techniques, membrane filtration, ion exchange, and adsorption (Fu and Wang, 2011). To date, considerable research attention has been paid to the removal of heavy metals from contaminated water via adsorption process. In theory, the adsorption process can offer flexibility in design and operation

*Corresponding author: Sreekanth. B
Department of Chemistry, SDMCET Dharwad.

and in many cases will produce high-quality treated effluent. In addition, as the adsorption is sometimes reversible and adsorbent can be regenerated by suitable desorption process, various types of adsorbents have found application in the removal of heavy metals, including activated carbon, carbon nanotubes, polymeric adsorbents, metal oxides, and bio-adsorbents. Among these adsorbents, iron-based magnetic nanoparticles have distinguished themselves by their unique properties, such as larger surface area-volume ratio, diminished consumption of chemicals, and no secondary pollutant. However, with another special property of this kind magnetic materials are realized and utilized in the context of environmental remediation. More and more magnetic separation has been combined with adsorption for the removal of heavy metals from contaminated water at laboratory scales. Especially in industries, magnetic separation is desirable because it can overcome many drawbacks occurring in the membrane filtration, centrifugation, or gravitational separation and is easy to achieve a given level of separation just via external magnetic field. Iron oxides exist in many forms in nature, with magnetite (Fe_3O_4), hematite (α - Fe_2O_3) and maghemite (γ - Fe_2O_3), being most probably common and important technologically (Teja and Koh, 2009). It has been reported that surface effects have a strong influence on the magnetic properties of iron oxide nanoparticles (Neuberger, *et al.* 2005). As the surface area of iron-oxide-based magnetic materials decreased, their responses to external magnetic field decreased, making it difficult to recover the adsorbents after treatment has been completed. On the other hand, it has also been noted that the adsorption capacities of adsorbents rely largely on the available surface areas, and the increase of the surface area is normally obtained by the decrease of the particle size of adsorbents. As a result, there is a need to synthesize such adsorbents with proper particle sizes for the removal of heavy metals from industrial wastewater. Up to now, there are several methods that can be used to synthesize iron-oxide-based nanoparticles. These methods include hydrothermal synthesis, thermal decomposition, co-precipitation (Yu, *et al.* 2006). sol-gel method and colloidal chemistry method. Among these synthesis methods, co-precipitation has proven to be the most promising method for the production of nanoparticles as the procedure is relatively simple and the particles can be obtained with controlled particle size.

MATERIALS AND METHODS

Materials

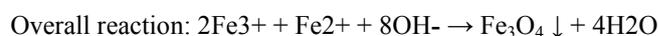
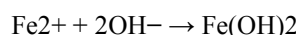
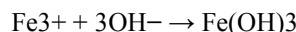
All the chemicals were of analytical reagent grade and used without further purification. Ferrous sulphate ($FeSO_4$, 99%), Ferric chloride ($FeCl_3$, 99%) and Sodium hydroxide (NaOH) for the synthesis of nanoparticles. Copper sulphate pentahydrate ($CuSO_4 \cdot 5H_2O$) and Potassium dichromate ($K_2Cr_2O_7$) for the batch adsorption studies.

Synthesis of Fe_3O_4 Nanoparticles

Iron oxide nanoparticles are synthesized using Co-precipitation method. This method is probably the simplest and most efficient chemical pathway to obtain magnetic nanoparticles. Iron oxides (Fe_3O_4) are usually prepared by dissolving stoichiometric mixture of ferric ($FeCl_3$) and ferrous (Fe_2O_3) salts in aqueous medium with a ratio of 2:1 (Fe^{3+}/Fe^{2+}). 100ml of 0.4mol/L solution of $FeCl_3$ and 100ml of 0.2mol/L solution of Fe_2O_3 were mixed and dissolved in distilled water.

Then 2mol/L of Sodium hydroxide (NaOH) was added into the above solution and the pH value was maintained between 10-11 with continuous stirring using a magnetic stirrer for 1 hour and a dark black precipitation was formed. The produced precipitation was filtered & after drying at 150°C for 2 hours, about 4.75 grams of Fe_3O_4 nanopowder is obtained. Particles with sizes ranging from 5 to 100nm will be obtained using this method.

The possible chemical reactions for the formation of Fe_3O_4 may be written as



The reaction is fast, very high yielding and Fe_3O_4 crystals are seen instantaneously after the addition of NaOH to the solution mixture of ferric chloride and ferrous sulphate.

RESULTS AND DISCUSSIONS

Characterization

Scanning Electron Microscopy

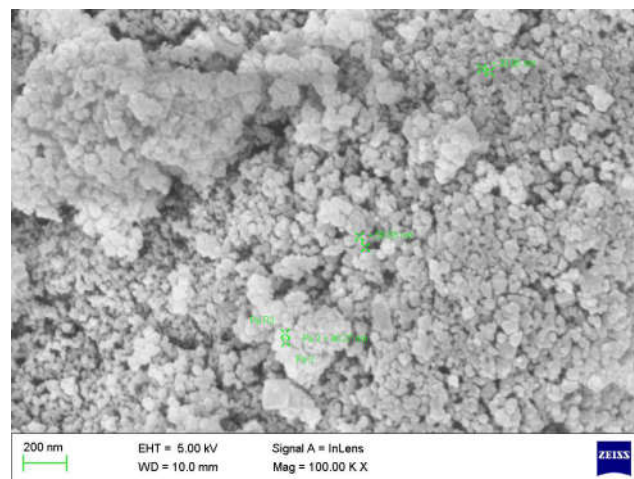


Figure 1. SEM image for Fe_3O_4 Nanoparticles

The SEM was analyzed using Ultra 55 FESEM, Carl Zeiss equipment using different magnifications from 25KX to 100KX. The SEM images for the iron oxide (Fe_3O_4) nanoparticles as shown in the Figure-12, confirms that the Fe_3O_4 nanoparticles are having spherical shape. The average particle size from the figure is 45nm. The SEM was analyzed using Ultra 55 FESEM, Carl Zeiss equipment using different magnifications from 25KX to 100KX. The SEM images for the iron oxide (Fe_3O_4) nanoparticles as shown in the Figure-12, confirms that the Fe_3O_4 nanoparticles are having spherical shape

X-ray powder Diffraction

XRD analysis confirmed that the synthesized nanoparticles were Fe_3O_4 as shown in Figure-2.

Six characteristic peaks were obtained at 30°, 35.05°, 42.69°, 53.07°, 56.55° and 62.19° reveal that the resultant black colored powder were Fe₃O₄ nanoparticles which matched well with the standard spectrum of Fe₃O₄ nanoparticles. In the pattern of XRD result, Sharp peaks suggest that the Fe₃O₄ nanoparticles have good crystallize structure and the broad nature of the diffraction bands indicated that nanoparticles have small particle sizes.

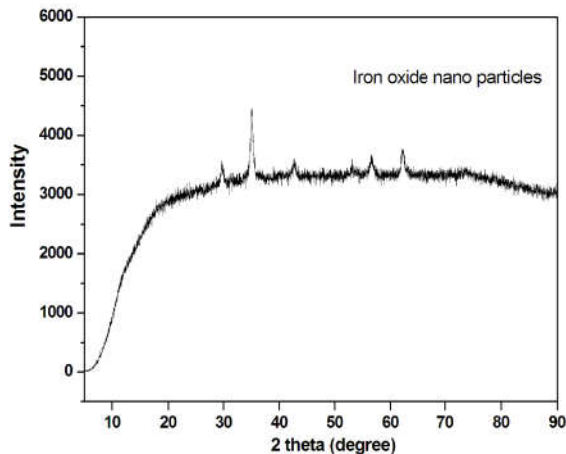


Figure 2. XRD graph for Fe₃O₄ Nanoparticles

The CuK α radiation with a wavelength ($\lambda=0.154\text{nm}$) was used to calculate the particle size as recorded in Table-1. The particle sizes can be quantitatively evaluated from the XRD data using the Debye – Scherrer equation given by,

$$D_p = \frac{0.94\lambda}{\beta_{1/2} \cos \theta}$$

Where, D_p = Particle size (in nm)

β = Line broadening (FWHM) (in degrees)

θ = Bragg angle (in degrees)

λ = X-ray wavelength (in nm)

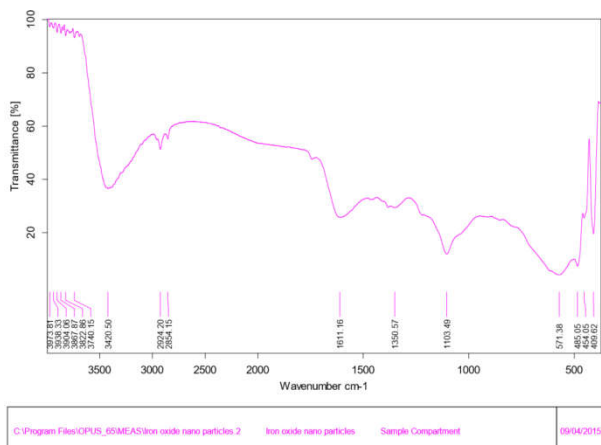


Figure 3. FTIR graph for Fe₃O₄ Nanoparticles

Fourier Transform Infrared Spectroscopy

The successful synthesis of iron oxide nanoparticles were confirmed by FTIR measurements between 4000cm⁻¹ to 400cm⁻¹. The various absorption bands obtained by the graph (Figure-14) have been utilized for the characterization of Fe₃O₄ nanoparticles.

The obtained peaks matched well with the standards. The presence of absorption peak at 571.38 cm⁻¹ corresponds to the Fe-O vibration. The peak at 3420.60 cm⁻¹ corresponds to the (HO-H) stretching. The peak at 1611.16 cm⁻¹ corresponds to the (HO-H) bending.

Batch studies

The experiments for the reduction of Copper(II) and Chromium(VI) was performed in the DO bottles into which aqueous solution of metal ions (Cu⁺² and Cr₂O₇⁻²) was taken from their stock solution. Then the synthesized Fe₃O₄ nanoparticles were added. These bottles were kept for stirring using mechanical shaker. Different parameters were studied and metals were analyzed using UV-VIS spectrophotometer.

Effect of pH

The pH was adjusted by adding 0.1 M HCl and 0.1 M NaOH solutions into the distilled water. Five solutions of different pH were prepared. 100mL of solutions containing 10ppm of metals were treated for 30 min with 0.1 g of nanoparticles at room temperature of 30°C. Initial absorbance was noted and kept them for continuous stirring using mechanical shaker. After 30 min, the final absorbance was noted and corresponding decrease in the conc. values are obtained.

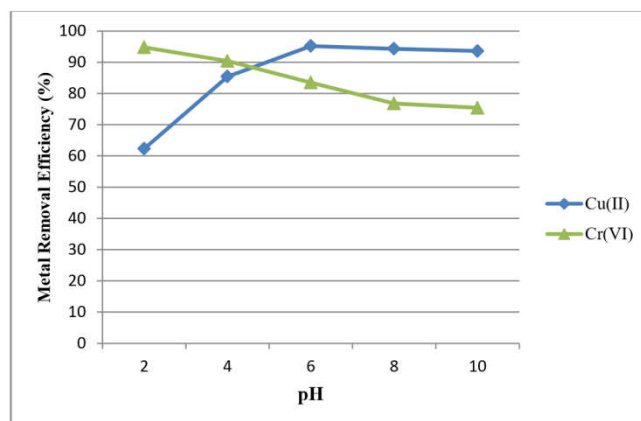


Figure 4. Effect of pH

The adsorption behavior under different pH shown from our results as well other results from previous authors indicated, in general, that there is electrostatic interactions between the adsorbent and the metal (adsorbates). According to the literature, it was indicated that the nanoparticle is positively charged at pH below 4.6, and negatively charged at pH above 4.6. This is due to the higher concentration of protons (H⁺) that surrounds the nanoparticles at low pH. Therefore, positive metal will have higher electrostatic repulsion with the adsorbent surface at lower pH and, as a result, the adsorption of positive metals will reduce. Increasing pH will decay the competition between H⁺ and the positive metals for surface sites and the adsorption of the positive metals with iron oxide nanoparticles will increase.

Effect of Contact time

The adsorption behavior under different pH shown from our results as well other results from previous authors indicated, in Time affects the adsorption of Copper (II) and Chromium(VI) ions to a great extent. By varying the values of time from 20 to 100 minutes and keeping other values constant i.e the of pH for Copper(II) to 6 and the pH for Chromium(VI) to 2, amount of nanoparticle dosage to 0.1 g, and concentration to 10ppm and

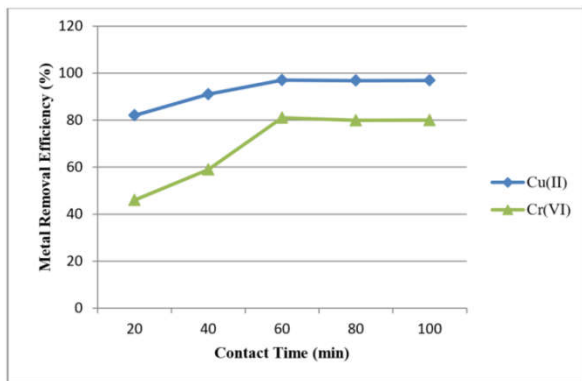


Figure 5. Effect of Contact time

the temperature to 30°C. Initial absorbance was noted and kept them for continuous stirring using mechanical shaker. At every 20 minutes, the absorbance was noted for Cu(II) & Cr(VI) and corresponding decrease in the concentration values are obtained. Fig.5 shows that at contact time of 60 minutes, the removal (%) was highest for both Copper(97%) and Chromium(81%).

Effect of Iron oxide nanoparticle dosage

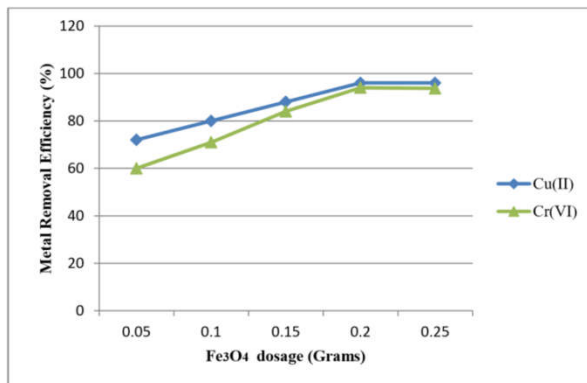


Figure 6. Effect of Iron oxide nanoparticle dosage

The adsorption efficiency increased with increasing the amount of nanoparticle (Fig.25). This is due to increase in surface area where the adsorption takes places. Different amounts of iron oxide nanoparticles are added from 0.05g to 0.25g to five aqueous solutions of heavy metals. About 0.2g of the iron oxide nanoparticles was enough to remove about 96.5% of Cu(II) and 94.5% of Cr(VI) at concentration to equal 10ppm for both metals, pH=6 (Cu(II)) and pH=2 (Cr(VI)), at temperature of 30°C and contact time of 60minutes.

Effect of Metal Concentration

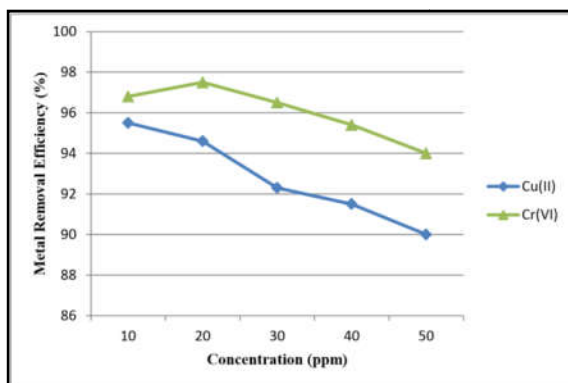


Figure 7. Effect of Metal concentration

Increasing the metal concentration results in the decrease in the metal removal efficiency (Fig.26). Maximum percentage removal was obtained at 10ppm for Copper(II) (95.5%) and 20ppm for Chromium(VI) (97.5%) by keeping other values as constant i.e pH=6 (Cu(II)) and pH=2 (Cr(VI)), contact time of 60minutes, nanoparticle dosage of 0.2g and temperature of 30°C. The percent removals of metals as a function of temperature are shown in Fig.27.

As temperature is increased from 10 to 60°C, metal removal efficiency goes on increasing upto 95.7% for Copper (II) and 94.2% for Chromium(VI) by keeping other values as constant i.e pH=6 for Copper(II) & pH=2 for Chromium(VI), contact time of 60 minutes, nanoparticle dosage of 0.2g, metal concentration of 10ppm for Copper(II) & 20ppm for Chromium(VI).

Adsorption isotherms

Langmuir isotherm for Copper (II)

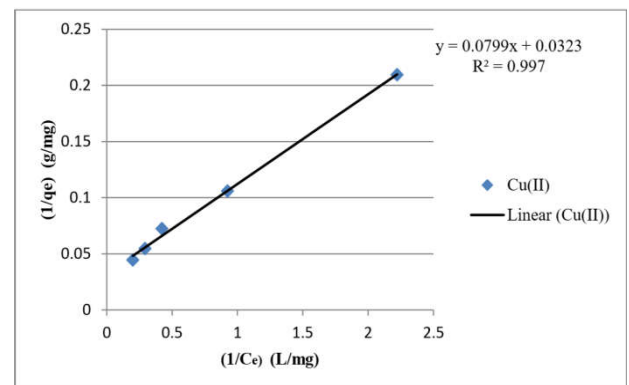


Figure 9. Langmuir isotherm for Copper (II)

From the graph (Fig.9), maximum adsorption capacity was $Q_0 = 31.25$ mg/g. Langmuir adsorption constant was $K_L = 0.405$ L/mg

Langmuir isotherm for Chromium (VI)

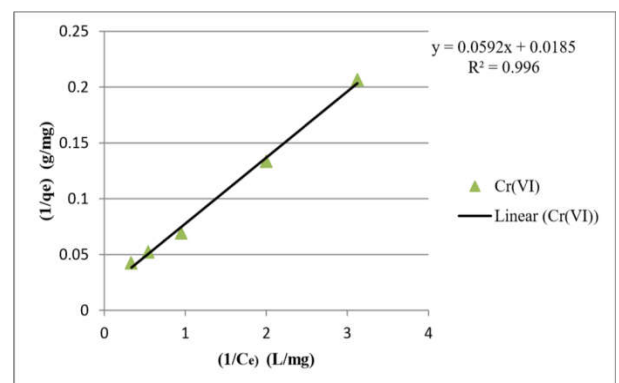


Figure 10. Langmuir isotherm for Chromium(VI)

From the graph (Fig.11), the adsorption intensity is $n=1.23$ which should lie between 1-10 for a favorable adsorption. The Freundlich isotherm constant is $K_f = 6.56$ mg/g.

Freundlich isotherm for Copper (II)

From the graph (Fig.11), the adsorption intensity is $n=1.23$ which should lie between 1-10 for a favorable adsorption. The Freundlich isotherm constant is $K_f = 6.56$ mg/g.

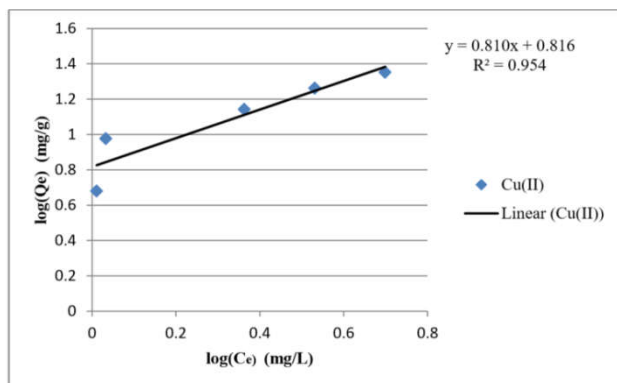


Figure 11. Freundlich isotherm for Copper (II)

Freundlich isotherm for Chromium (VI)

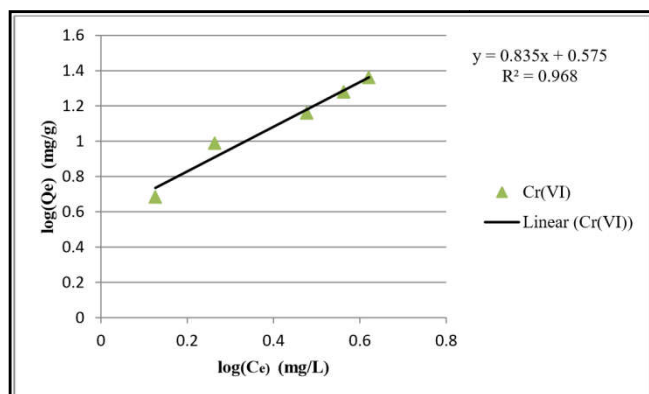


Figure 12. Freundlich isotherm for Chromium (VI)

From the graph (Fig.12), the adsorption intensity is $n=1.19$ which should lie between 1-10 for a favorable adsorption. The Freundlich isotherm constant is $K_f = 3.75\text{mg/g}$.

Conclusion

Iron oxide (Fe_3O_4) Nanoparticles were synthesized with the particle size ranging between 8.69nm-56.58nm (<100nm). The size and shape of Fe_3O_4 nanoparticle was confirmed using SEM, XRD and FTIR. Batch studies were conducted for the removal of toxic Heavy metals like Copper(II) and Chromium(VI). According to the results, maximum metal removal Efficiency (%) for Cu(II) and Cr(VI) were obtained at: pH=6 for Cu(II) and pH=2 for Cr(VI); Contact time=60minutes; Fe_3O_4 dosage=0.2g; Temperature=30°C; Metal concentration=10ppm for Cu(II) & 20ppm for Cr(VI). According to the pH effect, the mechanism of adsorption of Cu(II) and Cr(VI) was electrostatic interactions between the iron oxide nanoparticles and the heavy metals.

The Adsorption data fitted for both Langmuir and Freundlich isotherms out of which Langmuir Adsorption model was found to have the highest regression value of $R^2=0.997$ (Cu-II) & $R^2=0.996$ (Cr-VI) hence the best fit and acceptable. The maximum adsorption capacity (Q_0) for Copper(II) and Chromium(VI) from Langmuir isotherm model was determined to be 31.25mg/g and 55.56mg/g respectively.

REFERENCES

- Al-Saad, K. A. *et al.* 2012. "Iron oxide nanoparticles: applicability for heavy metal removal from contaminated water", *Arab Journal of Nuclear Sciences and Applications*, 45 (2), pp. 335-346.
- Chowdhury, S. R. and Yanful, E.K. 2010. "Arsenic and chromium removal by mixed magnetite-maghemite nanoparticles and the effect of phosphate on removal", *Journal of Environmental Management*, pp.2238-2247.
- Dada, A.O *et al.* 2012. "Langmuir, Freundlich, Temkin and D-R Isotherms Studies of Equilibrium Sorption of Zn^{2+} Unto Phosphoric Acid Modified Rice Husk", *IOSR-JAC*, Volume 3, Issue 1, pp. 38-45.
- Fu, F. and Wang, Q. 2011. "Removal of heavy metal ions from astewaters: a review," *Journal of Environmental Management*, vol. 92, pp. 407– 418.
- Neuberger, T., Schöpf, B., Hofmann, H., Hofmann, M. and Von Rechenberg, B. 2005. Superparamagnetic nanoparticles for biomedical applications: possibilities and limitations of a new drug delivery system,"*Journal of Magnetism and Magnetic Materials*, vol. 293, pp. 483–496.
- Palanisamy, K. L. *et al.* 2013. "The Utility of Magnetic iron oxide nanoparticles stabilized by carrier oils in removal of heavy metals from wastewater", *International Journal of Research in Applied, Natural and Social Sciences*, Vol. 1, Issue 4, pp. 15-22.
- Prijic, S. and Sersa, G. 2011. Magnetic nanoparticles as targeted delivery systems in oncology. *Radiol. Oncol.* ,45, pp. 1–16.
- Teja A. S. and Koh, P. Y. 2009. "Synthesis, properties, and applications of magnetic iron oxide nanoparticles,"*Progress in Crystal Growth and Characterization of Materials*, vol. 55, pp. 22–45.
- Wu, Y., Zhang, J., Tong, Y. and Xu, X. 2009. "Chromium (VI) reduction in aqueous solutions by Fe_3O_4 -stabilized Fe0 nanoparticles", *Journal of Hazardous Materials*, pp.1640-1645.
- Yu, W., Zhang, T. J., Zhang, X., Qiao, L., Yang, and Y. Liu, 2006. "The synthesis of octahedral nanoparticles of magnetite,"*Materials Letters*, vol. 60, pp. 2998–3001.
